Sophie Wuyckens[1]
September, 03 2018

EN-STI-BMI

Impact of the beam losses on the feedthroughs of the SPS electrostatic septa

CERN summer student report

Supervisors :
Dr. Francesco Cerutti
Dr. Luigi Salvatore Esposito

Introduction

One of the most important issues with accelerators are the regular and accidental beam loss impacts. To anticipate them, scientists are developing accurate simulation of particle showers initiated by beam-machine interaction as well as reliable machine model. In the context of this project, we focus on the Super Proton Synchrotron[2] (SPS) and more specifically on its extraction system towards the North Area initiated by the electrostatic septa (ZS's). The SPS is the second-largest machine in CERN's accelerator complex. It takes particles from the Proton Synchrotron and accelerates them to provide beams for the Large Hadron Collider[3], the North Area, the HiRadMat test facility[4] and AWAKE experiment[5] as shown in fig. 1.

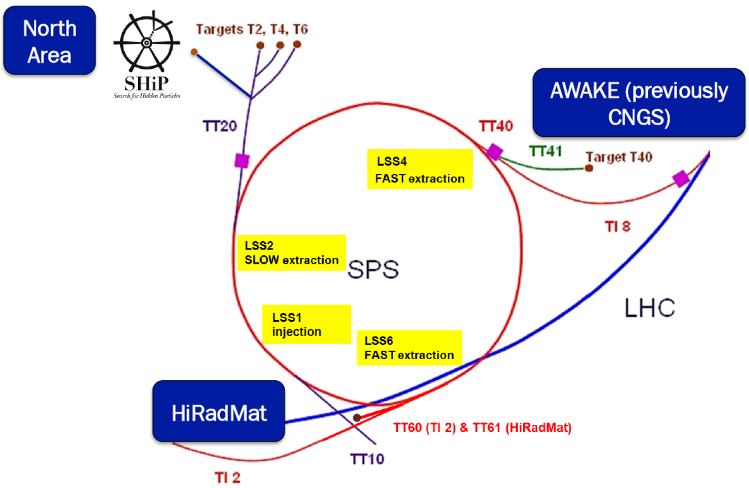

Figure 1: SPS complex[6]

The first part of the project consisted in the implementation of new prototypes still missing in the collection of elements available in the FLUKA geometry while the second part was aiming to a realistic case of beam losses induced by the mechanism of extraction of the SPS, serving to highlight its impact on the concerned machine segment, in particular the feedthroughs of the electrostatic septa.

[1]CP3, Université catholique de Louvain, Belgium
[2]`https://home.cern/fr/about/accelerators/super-proton-synchrotron`
[3]`https://home.cern/fr/topics/large-hadron-collider`
[4]`https://espace.cern.ch/hiradmat-sps`
[5]`https://home.cern/fr/about/experiments/awake`
[6]`https://home.cern/cern-people/updates/2017/02/using-crystal-extract-beam`

1 Electrostatic septa

In particle accelerators, a septum separates two distinctive field regions in order to selectively deflect particle beams (see fig. 2). It is used for injection and extraction of the beam.

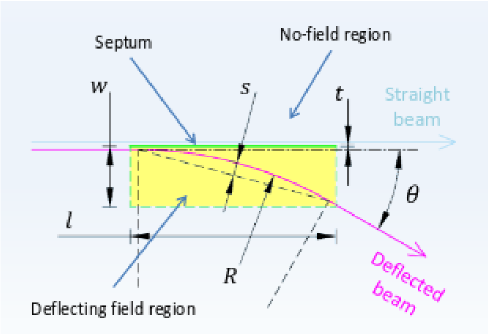

Figure 2: Basic principle of a septum
Courtesy of CERN Septa Section

With,
θ – Bending angle
R – Bending radius
s – Sagitta
w – Deflecting gap width
t – Septum thickness
l – Septum length

Since the septum that we are interested is electrostatic, it means that the extraction uses electric force to deflect particle of θ_c angle. Electrostatic bending angle θ_c of particles with single elementary charge is given by :

$$\theta_c = \frac{E \cdot l_{eff}}{10^9 \cdot \beta \cdot p} = \frac{U \cdot l_{eff}}{10^9 \cdot \beta \cdot p \cdot d} \tag{1}$$

with E, the electrical field.

In our case, the electrostatic septum consists in anode wires. The electric field is created between these septa and the cathode whose high voltage is powered by the so-called feedthrough.

2 Study case

The primary goal of this research is to give a complete simulation study to the TE/ABT group, for helping them to decide if the lead blocks located between each ZS's as presented on fig. 3 are useful or not to prevent the feedthroughs from the beam losses.

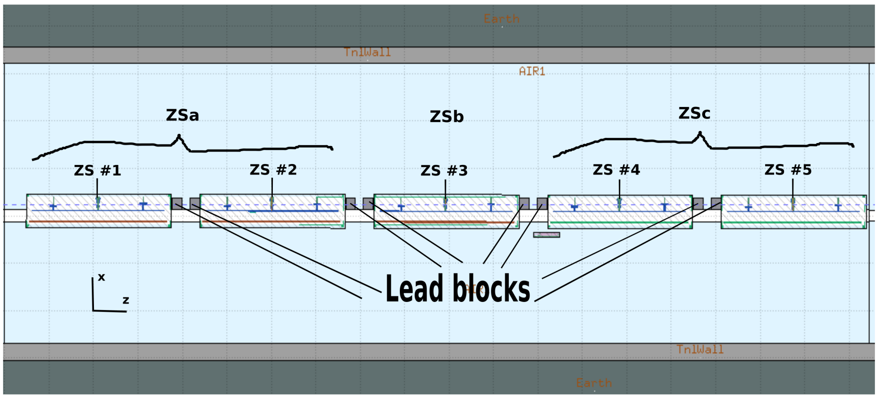

Figure 3: Geometry of the SPS ZS segment realized with $FLUKA$
@Original geometry of the ZS model made by **Daniel Björkman**

In order to solve this issue, simulation tests were performed with the $FLUKA$[7] software. The quantities studied were the energy deposition, particle fluence and dose in the different ZS's by

[7] http://www.fluka.org/

using dedicated scoring cards. Several shielding configurations were tested by changing the material but also the geometry of the blocks. In terms of the model, one has to take into account that the wires are modeled as a 200μm-ribbon perfectly aligned. The ribbon approximation has already been investigated and showed that it won't bring errors for our purpose. However, some evidence demonstrate that there is no perfect alignment among the wires although we are only interested in the relative effect between scenarios with/without lead blocks and one does not expect a big difference.

Moreover, the final choice (keeping or not the lead blocks) is influenced by the dose taking during an intervention. A previous study[7] shows the contribution of each component to the residual dose rate and is shown in fig. 4. This comparison does not take full complexity of the geometry into account.

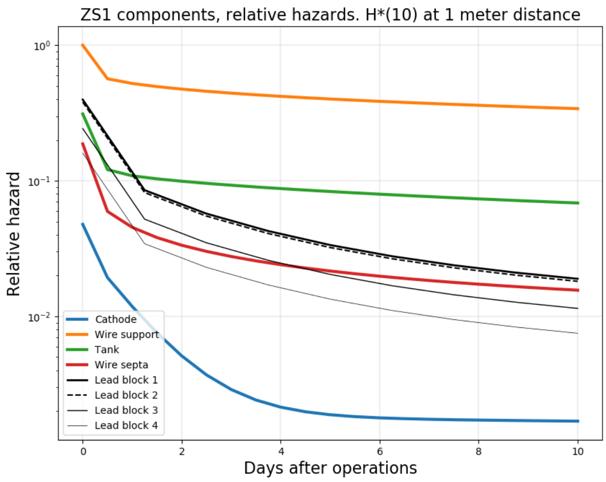

Figure 4: Hazard of lead blocks compared to hazards for ZS #1
From **Daniel Björkman** slides[8]

The wire holder is clearly the largest contributor to the hazard. However, the wire septa and tank material also contribute significantly while the lead blocks contribute to short term radiological hazard. This last feature cannot be ignored in the case for example if one wants to remove the lead blocs while replacing a ZS, especially in the first two days after operations of the beam.

3 Simulation model

Generally, to model the particles behaviour in an accelerator complex with an extraction system such as an electrostatic septum, one has to look at the phase space. The idea is to run the beam onto a slow-resonance using extraction sextupoles that cause the particles in the beam to move in an unstable but controlled way and peel off the unstable particles using an electrostatic septum that deflects them towards the extraction line. This is called "resonant extraction". Fig. 5 shows the distribution of the 400 GeV/c protons for the last 4 turns :
These protons can follow three distinct paths :

1. **Circulating** in the accelerator
2. **Extracted** : one of the separatrix of the distribution is intercepted by the septum wires that extract the beam. This is called the 1/3rd integer extraction
3. **Impact** on wires : particles might interact and generate energy deposition

[8] https://indico.cern.ch/event/744318/

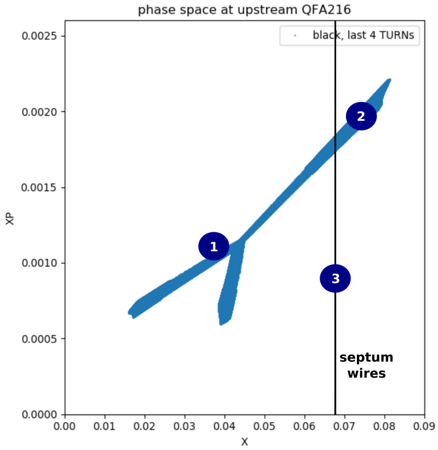

Figure 5: Black distribution by **Linda Stoel**

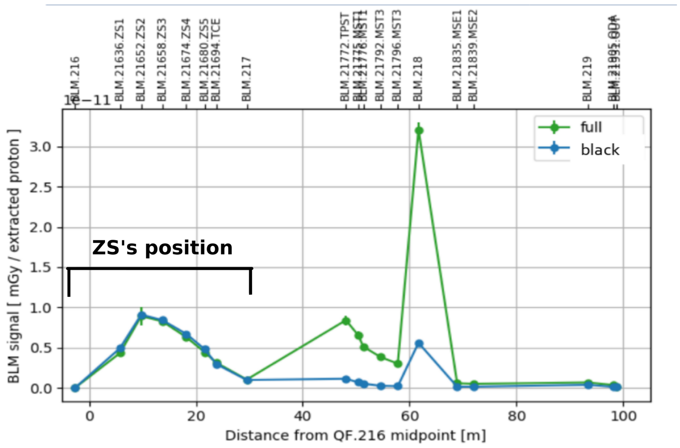

Figure 6: Dose received in Beam Loss Monitors

This *black* distribution does not take into account neither the multi-turn or the scattering process in the wires as the *full* one, however according to a former study[9], no large differences are expected for ZS as shown in fig. 6.

4 Modification of ZS prototypes

The ZS model was adapted to have a more accurate representation of the feedthroughs. Firstly, at the center of the feedthrough, a copper wire has been added. Secondly, the shape of the insulator has been detailed to cover the whole feedthrough and contain the copper wire. The aluminum shell was already there. The result is shown in fig. 7

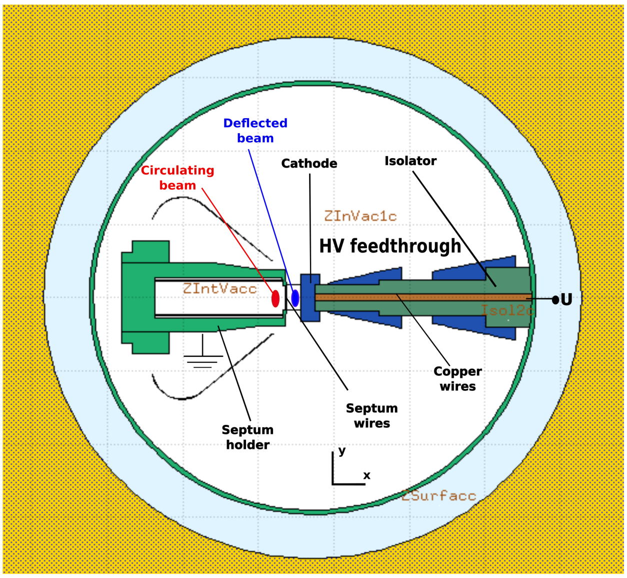

Figure 7: View of one of the ZS prototype in plan x-y

5 Energy deposition

In this section, we look at the energy deposition in several targets of interest in each ZS's.

[9]https://indico.cern.ch/event/743702/

5.1 In all ZS regions

Firstly, we want to see which regions are the most impacted by the energy deposition and compare between the different ZS's. Fig. 8 summarizes this study for the 'without lead' case. The energy fraction is normalized with respect to the total energy of 400 GeV/c protons.

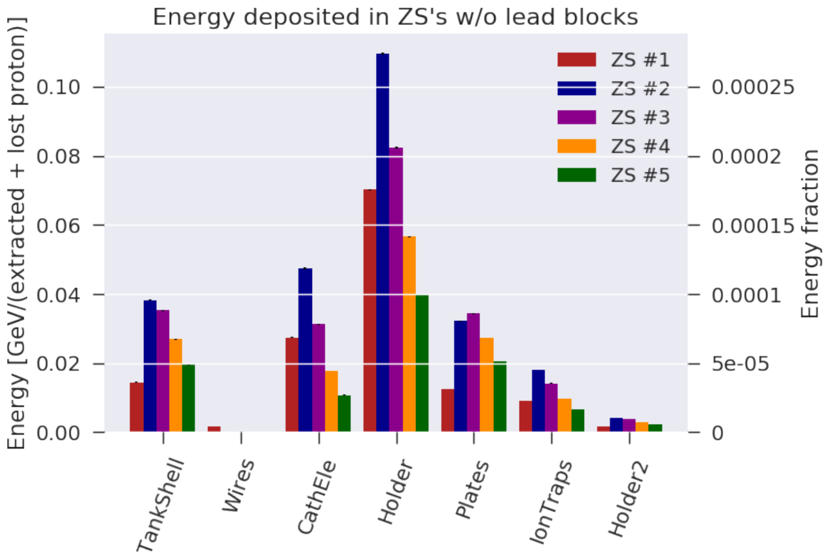

Figure 8

As for the previous study fig. 4, most of energy goes into the wire holders. In our model, protons hit an obstacle, the wires of the first ZS, in the first tens of centimeters and start to lose energy or be scattered by electromagnetic interactions. No energy is deposited in the wires of the next ZS since they are in the shadows of the first one. The propagation of the particle shower through the ZS's deposits the maximum energy in the second ZS and then decrease in the last ZS's.

5.2 In feedthroughs

The feedthroughs as mentionned previously are the power feeds of the cathode in the ZS and our main target of interest. It consists of an external aluminium shell covering an insulator with a copper wire at its center. Two cases are studied : with lead blocks and without them.

- **Black distribution**

  The energy deposition is scored in three regions for the five ZS's : Aluminum shell, insulator and copper wire. The results are summarized in fig. 9.

  As expected, the second ZS is the most impacted by the energy deposition. The percentages show the gain with repect to 'without lead blocks' case. We see that lead blocks won't reduce ZS #2 at the level of ZS #1 because its reduction factor is only around 5 - 10%. In addition, no differences are observed at the level of ZS #1 due to the fact there are no lead blocks shielding this element.

- **Black v.s. Full distribution**

  In order to quantity the difference between the black and the full distribution, a simulation was made by using both of these distributions. The quantities analyzed are the same as previously and are shown in fig. 10.

  These plots show that the black distribution is overestimating the energy losses by a factor 7-15%. This behaviour is due as discussed in section 3 to the fact that the full distribution

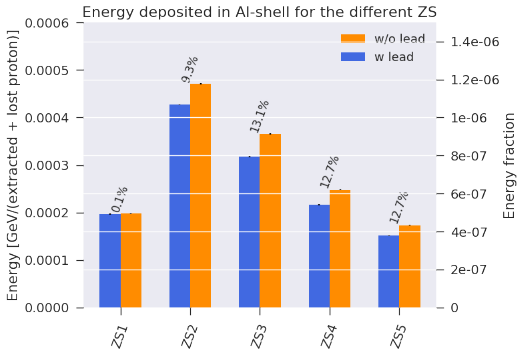

(a) Aluminium shell

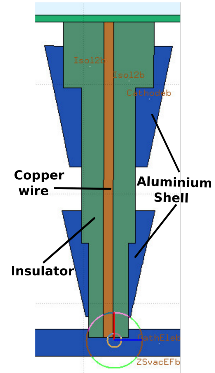

(b) Prototype

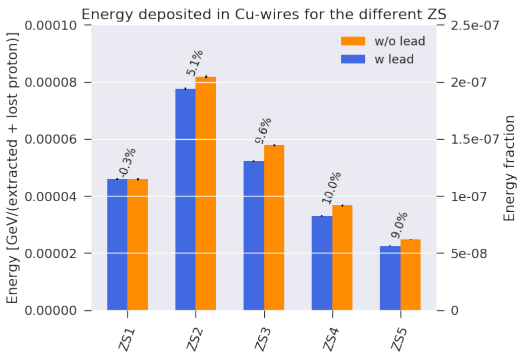

(c) Copper wire

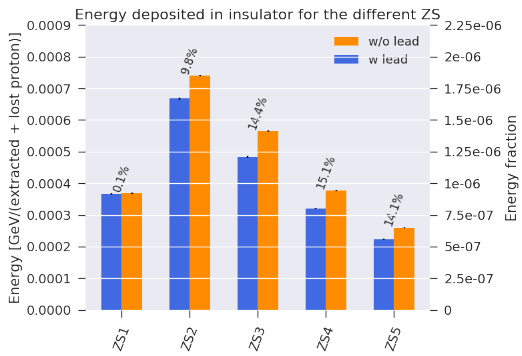

(d) Insulator

Figure 9: Energy deposited in feedthrough **with & without lead blocks**

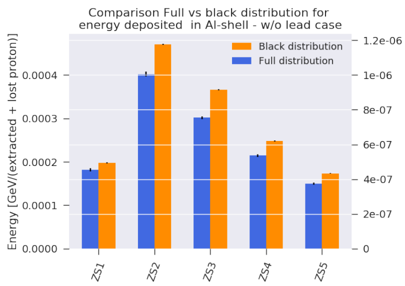

(a) Aluminium shell

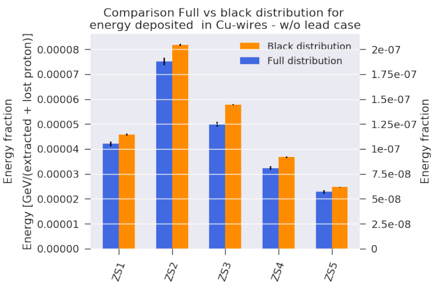

(b) Copper wire

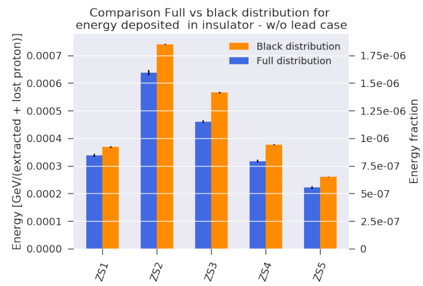

(c) Insulator

Figure 10: Energy deposited in feedthrough for the different ZS's - **Full v.s. Black**

takes into account the multiturn and scattering processes. It means for example that a particle might scatter and then manage to do a new turn in the accelerator. When it comes back to the extraction system, it does not have the same position as before and we can observe a dip in the linear density distribution at the position of the ZS wires.

5.3 Particle fluence

The starting point is the 400 GeV/c proton beam but when these protons are deviated from their initial trajectory to be extracted, they might hit the wires and interact with the medium. A particle shower follows this process and propagates in the other components of the ZS. A scoring of the particle fluence has been made in each regions of the feedthrough. Fig. 16a shows, as an example, the particle fluence in the third ZS in the insulator. Photons and electrons are the most abundant as expected because of the electromagnetic interactions that constitutes the biggest part of the shower. Fig. 16b-16c-16e compare the scenarios with and without the lead blocks for some of the shower particles. Theses results are consistent with what has been scored in terms of energy deposition with a gain around 10-15%.

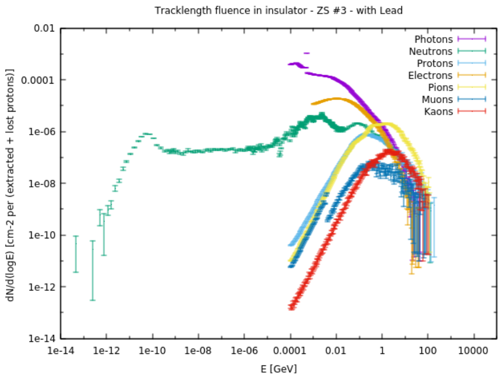

(a) All particles

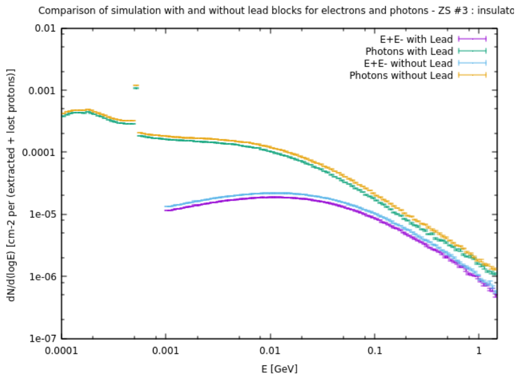

(b) Electrons and Photons - with and without lead

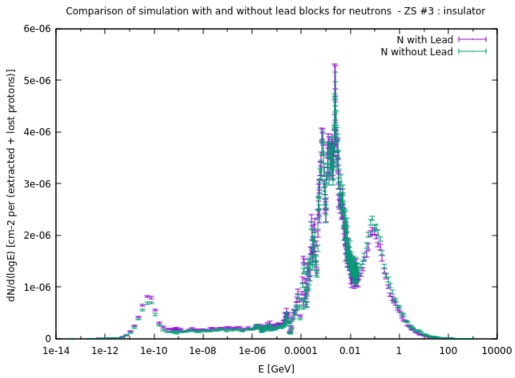

(c) Neutrons - with and without lead

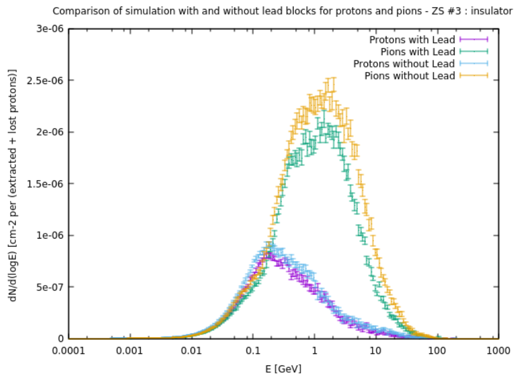

(d) Electrons and Photons - with and without lead

Figure 11: Particle fluence

The neutrons do not show any differences between both cases. This is an important feature given that neutrons are the particles that could contribute the most to the hazard though nuclear interactions.

5.4 Other shielding configurations

As a further investigation, we wanted to test other shielding configurations in terms of material and geometry of the blocks. The lead blocks used in the previous study are 204mm in length (x-axis) and 100 mm thick (y-axis) as shown in fig. 12a. The plots presented in fig. 12 give the reduction factor in energy deposition when taking the case without lead blocks as a reference. The nominal lead blocks (red bars) reduce energy deposited in the feedthroughs by 5-15% as described in section 5.2.
The first modification made was to use marble instead of lead (green bars) and led to a gain of ∼3 - 10% which is lower than the lead case. The orange bar stands for the case of lead blocks shortened to 156 mm to avoid the conflict with the red component on fig. 12a. This case seems even more useless compared to the previous ones with a gain of only ∼1 - 7%. Finally, if we double vertically the size of lead blocks with a thickness of 200mm, we see (in magenta) that this is somewhat the most efficient configuration (∼5 - 20%). However, we still have to take into account the fact that more lead means increase of the activation process which would contribute to short-term radiological hazard.

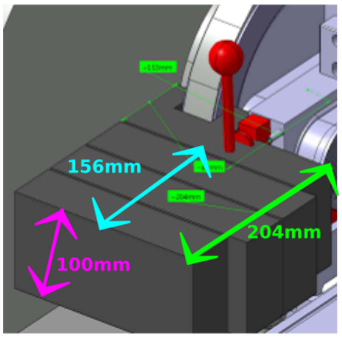

(a) Lead block geometry

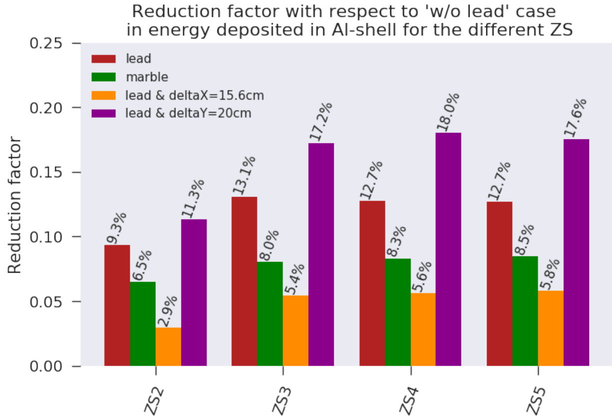

(b) Aluminium shell

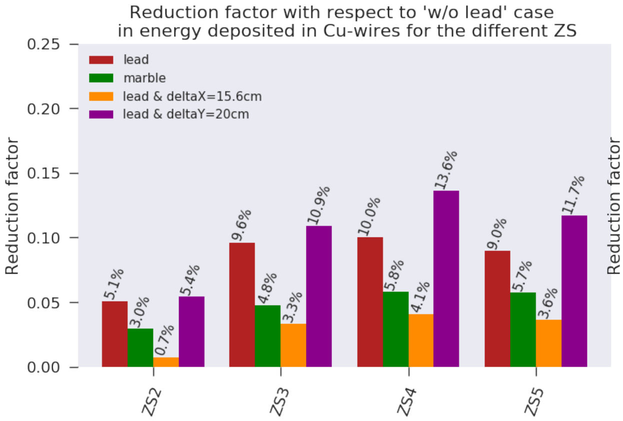

(c) Copper wire

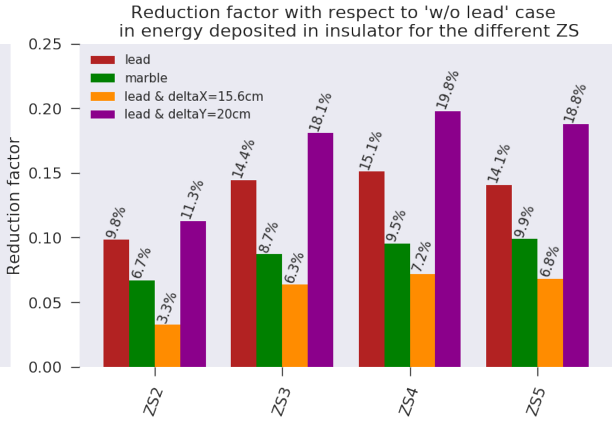

(d) Insulator

Figure 12: Gain obtained for different shielding configurations

6 Dose

The dose is another way to quantify the energy deposited in elements (in mass). We focused on the feedthrough and compared between the different shielding configurations.

By looking at fig. 13, one can see that the dose deposition in the feedthrough is highest near the cathode and drops off with increasing distance. The maximum dose received is about 3.5 MGy per 10^{19} protons (∼1 year of operation). The different shielding configurations do not make a significant difference as the plots in fig 14 suggest it.
In order to get a more accurate idea of the hazard this dose could represent, we made a comparison to a radiation hardness study for the CMS pixel cooling fluid[10]. In their experiment, they placed a disk made of beryllium in a jar containing the coolant, FC72 fluorinert, and exposed it to $2 \cdot 10^5 Gy$ of Co^{60} per cm^2. As a result, no differences were observed in the coolant properties which permit us to use their value as a limit. In our case, there is a also a coolant (FC77) inside the insulator of each feedthrough but we have a factor ∼10 more which means at first sight that the feedthrough could be compromised. However, it might be an overestimation mainly due to two factors : the coolant is not located at the peak point dose and the fluid is circulating and filtered. It is then reasonable to expect the feedthoughs to survive such doses, when taking into account that the total volume of coolant (50 l) is a factor 20 times higher than the volume of coolant flowing inside the feedthroughs (50 cl) because we

[10]M. Atac et al, Radiation hardness studies of cooling fluids epoxies and capacitors for CMS pixel system, Nucl. Instr. Meth. A, 476, 3, 2002, 676-679, `https://doi.org/10.1016/S0168-9002(01)01772-7`.

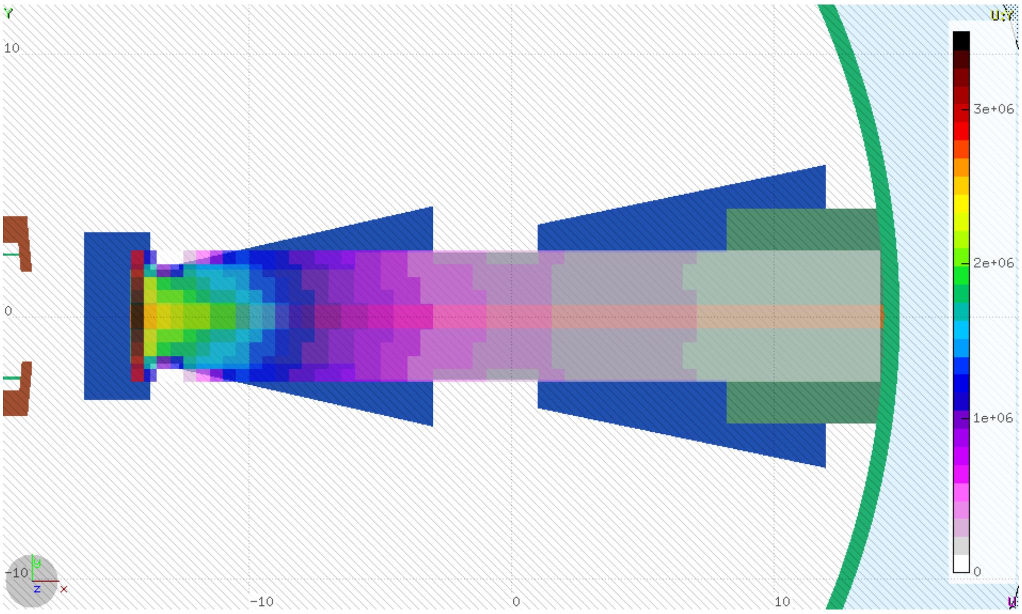

Figure 13: Dose deposition in ZS #2 - without lead

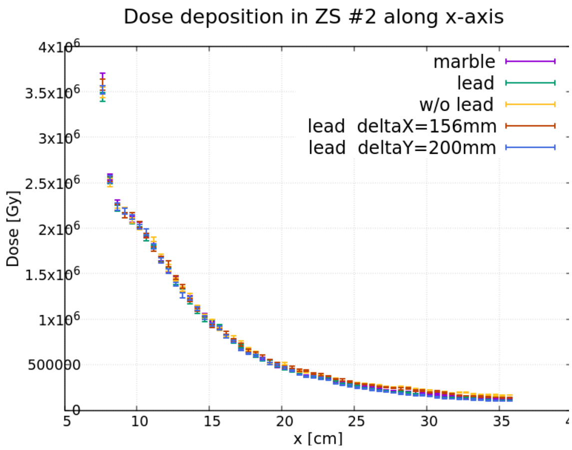

(a) Peak dose along x-axis

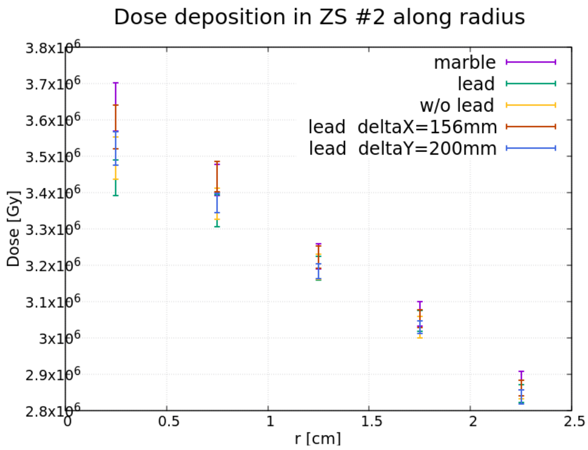

(b) Peak dose along radius

Figure 14: Peak dose deposition in feedthrough

have five ZS's.

7 Temperature increase

In this last section, the temperature increase in the ZS's is studied by converting the energy deposition scoring in the proper way.
To obtain the global temperature increase in $Kelvin$ from $\frac{GeV}{cm^3 \cdot \text{per proton simulated}}$, one has to apply the following formulas :

$$Norm_E(J/cm^3) = 10^9 \cdot 1.6 \cdot 10^{-19} \cdot I \cdot w \quad (2)$$

$$T[K] = \frac{Norm_E \cdot f_1(f_2)}{\rho \cdot C_p} \quad (3)$$

where,

- I = 10^{13} : Number of extracted protons

- Weight $= \frac{\text{simulated}p^+}{\text{lost-extracted}p^+} = 6.4$: Number of extracted and lost protons
- C_p : Specific heat capacity $[J/g \cdot K]$
- ρ : Density $[g/cm^3]$
- $f_1(f_2) = \frac{A_{wires}}{A_{ribbon}}$ - only for wires because of the ribbon approximation

7.1 Wires

If we focus on the septum wires (2080 wires 312 x 200 μm), the material is W-26Re with $\rho = 19.757 g/cm^3$, the specific heat of W-26Re is $C_p \sim 0.140 J/gK$ and others relevant parameters are listed in table 1. The temperature increase can reach 100 K in the first ZS which is the most exposed to the beam as shown in fig. 15.

	W-26Rea	W-26Rebc
Diameter	60 μm	100 μm
f	$\sim$106.45	$\sim$ 38.34
$Norm_T$	394091.06	141939.42

Table 1

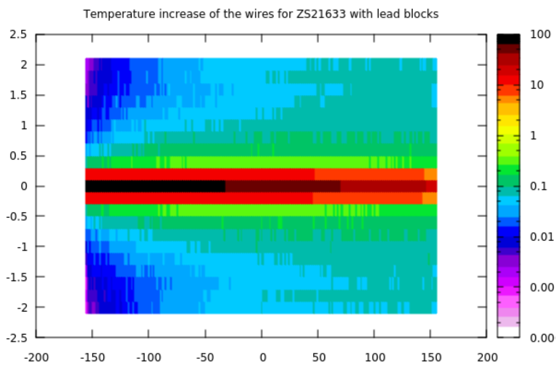

(a)

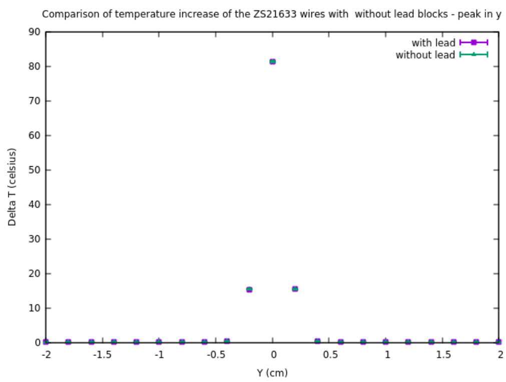

(b) Peak along y-axis

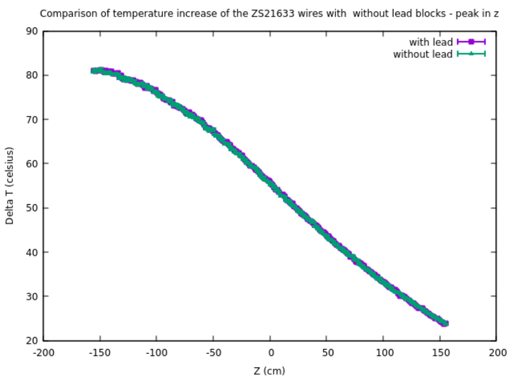

(c) Peak along beam-axis

Figure 15: Temperature increase in wires of ZS #1

As expected, fig. 15b-15c show no apparent differences between the scenarios with and without lead blocks.

7.2 Septum holder

The temperature increase in the support of the wires has also been investigated. It is made of stainless steel SS304L material with $\rho = 8.02g/cm^3$ and specific heat of $C_p \sim 0.502416J/gK$. The scoring was divided in two with the upper and lower septum holder for more accuracy. Fig. **??**-16 show that the temperature increase in the anode support due to particle showers is only a few tens of millikelvins, and thus insignificant.

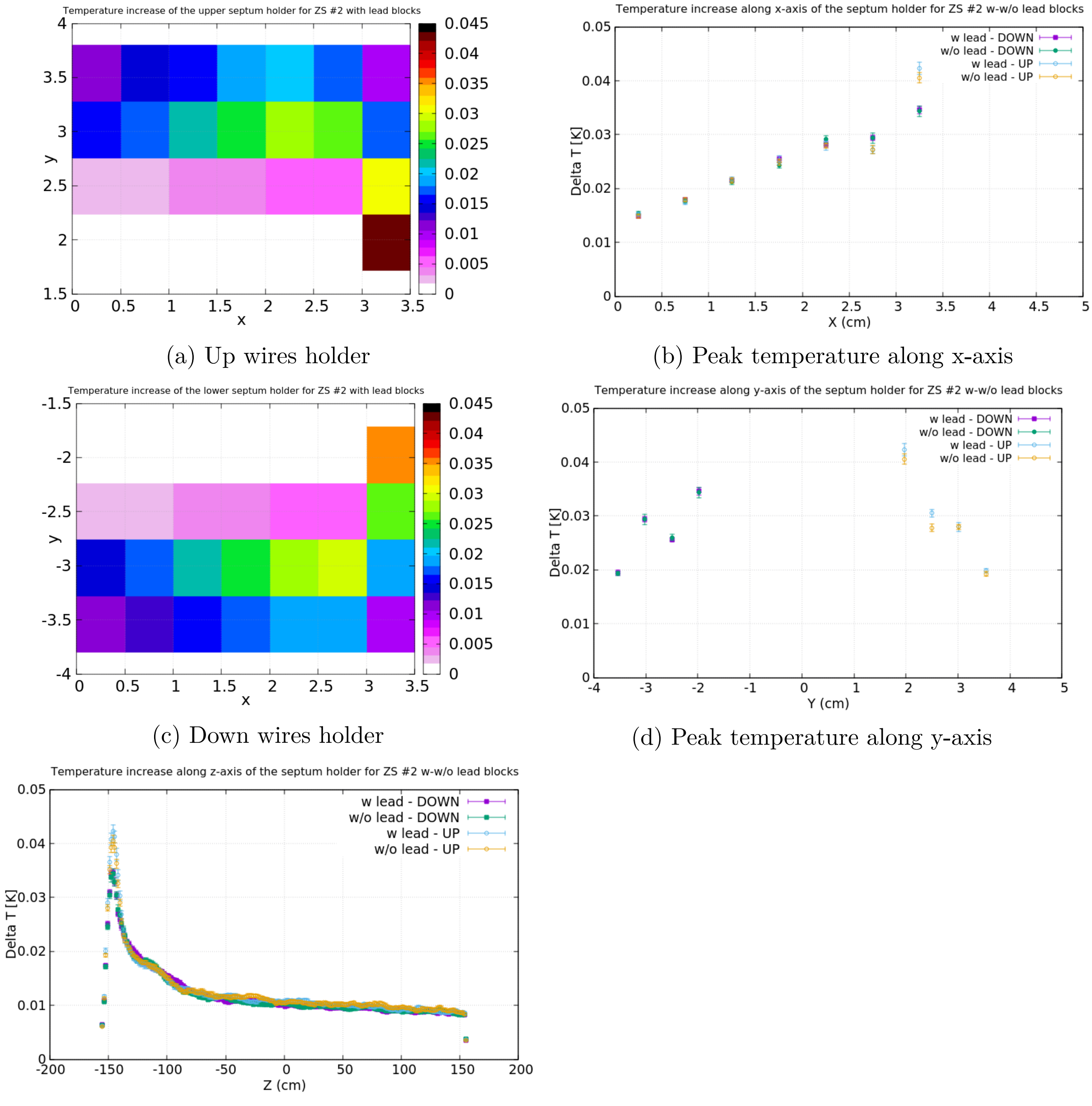

(a) Up wires holder

(b) Peak temperature along x-axis

(c) Down wires holder

(d) Peak temperature along y-axis

(e) Peak temperature along z-axis

Figure 16: Temperature increase peak of the wires support of ZS #2

7.3 Feedthrough

Another scoring has been made on the feedthrough. Since the bins of the scoring overlap several material, highest density material was chosen for the calculations. We consider then the material as Copper with $\rho = 8.96g/cm^3$ and the specific heat : $C_p \sim 0.385J/gK$
Fig. 17 shows that the adiabatic temperature increase is less than 0.008 K. The temperature raised mainly at the center of the feedthrough near wire and towards the cathode element

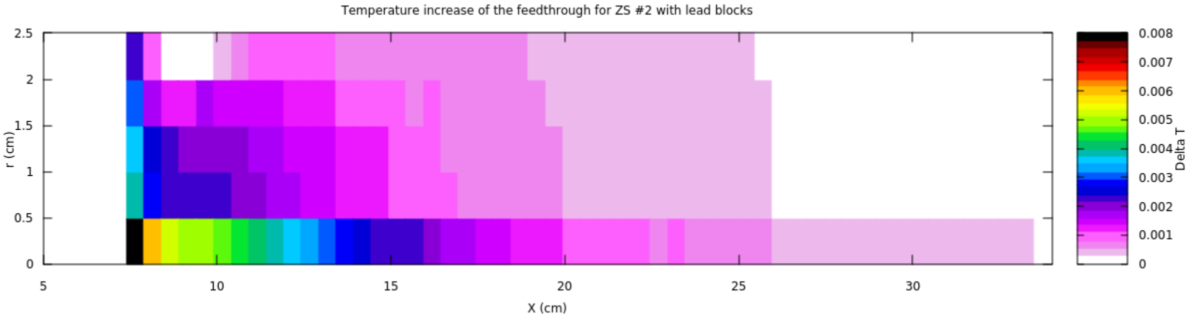

Figure 17: Temperature increase of the feedthrough of ZS #2

which makes sense since it's closer to the beam.

Conclusion

The shielding efficiency of the lead blocks protecting the ZS feedthroughs was studied, using the FLUKA model with the ZS wires modelled as density corrected 200 um ribbons and an non-scattered source term, and scoring energy deposition, particle fluence and dose.
After showing these results at the SLAWG meeting #34[11], the TE/ABT group decided that since the lead blocks make such a small difference for the feedthroughs, they should be taken out.

[11]https://indico.cern.ch/event/748453/